European Journal of Pharmaceutics and Biopharmaceutics 74 (2010) 184–192

Contents lists available at ScienceDirect

European Journal of Pharmaceutics and Biopharmaceutics

journal homepage: www.elsevier.com/locate/ejpb

Research paper

Size-dependent release of fluorescent macromolecules and nanoparticles from radically cross-linked hydrogels

Matthias Henke, Ferdinand Brandl, Achim M. Goepferich, Joerg K. Tessmar *

Department of Pharmaceutical Technology, University of Regensburg, Regensburg, Germany

ARTICLE INFO

Article history:
Received 31 March 2009
Accepted in revised form 25 August 2009
Available online 15 September 2009

Keywords:
Thermally cross-linkable
Hydrogel
Nanoparticle
Macromolecular drugs
Characterization
Release
FRAP

ABSTRACT

Hydrogels play an important role in drug delivery and tissue engineering applications due to their excellent biocompatibility and their variable mechanical and physical properties, which allow their optimization for many different aspects of the intended use. In this study, we examined the suitability of poly(ethylene glycol) (PEG)-based hydrogels as release systems for nanometer-sized drugs or drug carriers, like nanoparticles, using the radically cross-linkable oligo(poly(ethylene glycol)fumarate) (OPF) together with two cross-linking agents. Different fluorescent nanoparticulate probes with respect to size and physical structure were incorporated in the cross-linked hydrogels, and the obtained release profiles were correlated with the physical properties and the chemical structure of the gels, indicating a strong dependence of the release on the chosen PEG prepolymers. The prepared hydrogels were characterized by oscillatory rheometry and swelling experiments. Release experiments as well as diffusion measurements using fluorescence recovery after photobleaching showed the great potential of this type of hydrogels for the preparation of adjustable release systems by altering the molecular weights of the used PEG molecules.

1. Introduction

Hydrogels are widely used materials for drug delivery systems and as scaffolds for tissue engineering approaches due to their excellent biocompatibility, founded in their high water content, and their very flexible chemical and physical properties [1]. *In situ* cross-linkable oligomers, like oligo(poly(ethylene glycol)fumarate) (OPF), or other unsaturated poly(ethylene glycol)-based oligomers, e.g. acrylates, offer the possibility to easily adapt their chemical and physical properties by varying the distance between the unsaturated bonds or by using different types and amounts of added cross-linkers, such as poly(ethylene glycol) diacrylate (PEG-DA) or N,N′-methylene bisacrylamide (BIS) [2–5]. Furthermore, the radically cross-linkable oligomers can be used to prepare hydrogels with other chemical functionalities, like short cell adhesion peptides (e.g. Arg-Gly-Asp (RGD)) to enhance cellular adhesion or additional binding sites for growth and differentiation factors, which can both be introduced by mono-acrylated peptides or more sophisticated functional spacers [6,7]. Especially for tissue engineering applications, the controlled delivery of soluble bioactive substances, such as growth factors or plasmids for gene delivery approaches, can be seen as a key to success [8]. If a controlled release during these applications is intended, the exact timing of the release and the released drug amounts are crucial for the restoration of the damaged tissue, as cultured cells often need to be exposed to stimuli in an accurately timed fashion, which can range from days to weeks depending on the desired cellular effects [9].

A similar well-timed release scheme is necessary for hydrogels used in drug delivery applications, where hydrogels can control the release of bioactive molecules over longer time frames not only at specific locations, but also for a systemic delivery from locally applied drug depots [10,11]. Depending on the final application as controlled drug delivery system, one could think of three possible strategies to prepare radically cross-linked hydrogels with incorporated bioactive molecules. The first would be the direct entrapment of nanometer-sized bioactive substances (e.g. high molecular weight proteins) inside the hydrogel with a subsequent diffusion-controlled release, which can be further governed by external stimuli like the degree of swelling, changes in temperature or pH, a hydrolytic or enzymatic cleavage of network chains or individual cross-links, or a combination of all of these principles [12–15]. A second alternative for hydrogel release systems is the permanent entrapment of degradable or non-degradable polymeric particles within the gel network via chemical ligation or simply via physical fixation due to the small hydrogel mesh size. In this later case, the release of the embedded particles only proceeds with the breakdown of the hydrogel network, or alternatively, the individual drug

* Corresponding author. Department of Pharmaceutical Technology, University of Regensburg, 93040 Regensburg, Germany. Tel.: +49 941 9433286; fax: +49 941 9434807.
E-mail address: Joerg.Tessmar@chemie.uni-regensburg.de (J.K. Tessmar).

0939-6411/$ - see front matter © 2009 Elsevier B.V. All rights reserved.
doi:10.1016/j.ejpb.2009.08.011

molecules are slowly released from their depot inside the particles and subsequently freely diffuse through the hydrogel mesh in order to reach their site of action [16,17]. A possible third alternative is the combination of both release principles by simultaneously using free and encapsulated drug molecules, to allow the controlled release of two substances from the hydrogel-particle composite at the same time [18]. All the described release systems can be applied in the field of tissue engineering or drug delivery, but their applicability strongly depends on the intended drug substance and the clinical setting. Independent of the later application, it is of utmost importance to carefully characterize each developed system, since only the appropriate combination of mesh and drug substance is suited to provide a sufficiently prolonged release from the hydrogel matrix.

In this study, different hydrogels were prepared by radical polymerization of two types of OPFs made of different molecular weight PEG prepolymers. Furthermore, the polymers were reacted with different amounts and types of cross-linkers, which were chosen to produce a wide range of different hydrogel compositions. The increasing amount of cross-linker should furthermore elucidate the effect of a low molecular weight substance on the overall gel properties. The chosen cross-linkers were used in concentrations similar to those known from literature for bisacrylamide (e.g. 8% in literature [18,19]), but due to the smaller molecular weight of the used poly(ethylene glycol) diacrylate, it was used in significantly lower amounts than stated in literature for tissue engineering applications to keep the hydrogel defined mainly on OPF (33% in literature [20,21]). To investigate the controlled release solely based on the size of the investigated drug substances, no additional release systems, like for example gelatin particles, were incorporated in the gels, which is usually done in the studies known from literature and would furthermore complicate the investigation of the obtained release curves [18–20]. To investigate solely the size dependency, nanometer-sized model substances or nanoparticulate drug carriers were used in order to elucidate the network design criteria for future release systems. For this purpose, different fluorescent nanoparticles with respect to size and physical structure were incorporated in the afterwards cross-linked hydrogel-forming polymers, and the obtained release profiles were correlated with the determined physical properties and the chemical structures of the gels. The chosen dextrans should resemble typical drug substances applied in literature using hydrogels, like for example, insulin (5.7 kDa), TGF-β (44 kDa), immunoglobulins (∼150 kDa) or plasmid DNA (∼2000 kDa). For a rational design of suitable delivery systems in the future, exclusion limits and release profiles should be identified, which allow for a suitable retardation of active drug substances using the here described hydrogel materials. Application of the here described methods to other gel systems would furthermore also allow for the adjustment of the release profiles obtained with other hydrogel-forming oligomers.

2. Materials and methods

2.1. Materials

Ethyl acetate was purchased from Acros Organics (Geel, Belgium). Chloroform stabilized with 1% ethanol (HPLC grade) was obtained from Carl Roth GmbH (Karlsruhe, Germany). Deuterated chloroform was purchased from Deutero GmbH (Kastellaun, Germany). N,N,N′,N′-tetramethyl ethylenediamine (TEMED) was purchased from Fluka (Buchs, Switzerland). Poly(ethylene glycol) (3 and 10 kDa) was obtained from Hoechst (Frankfurt am Main, Germany). FluoSpheres® (2% dispersion, nominal diameter 100 nm) were purchased from Invitrogen GmbH (Karlsruhe, Germany). Dextran standards (M_n = 180; 342; 908; 3300; 8100; 18,300; 35,600; 100,000 and 236,000 Da) were purchased from PSS GmbH (Polymer standard service; Mainz, Germany). Ammonium persulfate, a higher molecular weight dextran standard (M_n = 410,000 Da), fluorescein isothiocyanate-dextrans (FITC-dextran) (4, 40, 500 and 2000 kDa), fumaryl chloride, N,N′-methylene bisacrylamide (BIS), poly(ethylene glycol) diacrylate (PEG-DA, M_n = 575 g/mol) and dibasic sodium phosphate were purchased from Sigma–Aldrich (Taufkirchen, Germany). Diethyl ether and methylene chloride were of technical grade and were used without further purification. 1 N NaOH solution, ortho phosphoric acid 85%, monobasic potassium phosphate, sodium azide, sodium chloride and toluene were obtained from Merck KG (Darmstadt, Germany).

A phosphate-buffered saline (320 mosmol) with higher buffering capacity than commercially available PBS was used for the cross-linking of the oligomers, it was prepared by dissolving 0.6 g monobasic potassium phosphate, 6.4 g dibasic sodium phosphate, 5.85 g sodium chloride and 250 mg sodium azide (for conservation) in 1 l purified water and was subsequently adjusted to pH of 7.4 using ortho phosphoric acid.

The purified water used for all experiments was obtained using a Milli-Q water purification system from Millipore (Schwalbach, Germany).

2.2. Synthesis of OPF oligomers

OPFs were synthesized starting from the differently sized PEG prepolymers (3 and 10 kDa) according to a procedure adapted from Jo et al. [2] without the addition of a base in order to avoid the formation of dark colored byproducts. For a typical reaction, 50 g of PEG was dissolved in toluene, and an appropriate amount of toluene was distilled off in order to remove any residual water using a Dean–Stark trap. A solution of an appropriate amount of freshly distilled fumaryl chloride (molar ratio PEG:fumaryl chloride 1:1.2) in anhydrous toluene was added dropwise under constant stirring at 50 °C in order to evaporate the formed hydrochloric acid. The reaction further proceeded for 2–3 days under permanent stirring at room temperature. To isolate the product, the solvent was removed by rotoevaporation. An excess of methylene chloride was added three times to the residue and rotoevaporated in order to completely remove toluene. The liquid residue was then dissolved in ethyl acetate and recrystallized twice in the freezer and was subsequently washed with ice-cold diethyl ether. The obtained oligomers were kept in a refrigerator at −20 °C until use to avoid cross-linking and degradation.

2.3. Characterization of OPF oligomers by ^{1}H NMR

For the ^{1}H NMR measurements, about 25 mg of the oligomer was dissolved in 1 ml deuterated chloroform. Spectra were recorded at 300 MHz with a Bruker NMR spectrometer Avance 300 (Bruker Elektronik, Rheinstetten, Germany) using tetramethylsilane as internal standard. All spectra were recorded at 300 K.

2.4. Characterization of OPF oligomers by GPC

For further characterization of the synthesized OPF oligomers, gel permeation chromatography (GPC) was performed using a Shimadzu LC-System consisting of a system controller (SCL-10A), a pump (LC-AT), a degasser (DGU-10B), an autosampler (SIL-10AD), a column oven (CTO-10AC) and a refractive index detector (RID-10A). A Phenomenex Phenogel 5 μm linear column (300 mm × 7.8 mm) was used for the analysis and kept at 40 °C during the experiments. About 100 mg of the oligomers was dissolved in 3 ml chloroform and filtered through a chloroform resistant syringe filter (0.2 μm) prior to use. Chloroform stabilized with 1%

ethanol was used as eluent. The flow rate for the experiments was preset at 1 ml/min. Molecular weights were determined using the GPC software for Class VP Version 1.00 from Shimadzu. The GPC calibration curve for the analysis was obtained by measuring the elution time of different PEG standards (M_n = 1080; 2000; 4120; 6450; 8500; 12,000; 20,000 Da).

2.5. Cross-linking of OPF hydrogels

Due to the incorporated double bonds of the fumarate groups in the OPF oligomers, they are cross-linkable via temperature- or UV-light-initiated radical polymerization [22]. In this study, the OPF oligomers were cross-linked using a water soluble cross-linking system consisting of ammonium persulfate as a radical initiator and TEMED as catalyst for the polymerization. In order to get a wide variety of hydrogels with different properties, like for example mesh size, stiffness or swelling behavior, different cross-linking agents and concentrations were used, similar to those known from literature. Table 1 gives an overview over the prepared hydrogel compositions used in this study.

2.6. Rheological characterization

For the investigation of the cross-linking reaction, the oligomer solutions according to Table 1 were prepared in ice-cold water and subsequently cast on the lower plate of an Advanced Rheometer AR2000 from TA Instruments (Eschborn, Germany), which was cooled to 5 °C in order to prevent an early cross-linking. The measurement was then started by heating up the sample to 37 °C. Time sweep measurements were conducted using a 40-mm steel plate (gap size of 1000 μm). A deformation of 1.000% and an oscillatory frequency of 1 Hz were preset for the instrument. The storage modulus G′ and the loss modulus G″ were recorded for 60 min. During all conducted experiments, a solvent trap was used to prevent drying of the hydrogel samples.

2.7. Swelling behavior of the hydrogels

In order to characterize the swelling behavior of the OPF hydrogels, gel cylinders were prepared by injection of an oligomer solution mixed according to Table 1 into a Teflon mold (each well had a diameter of 4.6 mm and a height of 15.4 mm). After cross-linking the oligomer solution at 37 °C for 1 h, the gel cylinders were removed from the mold and cut to equal lengths of 10 mm, except for the high molecular weight OPF10k composition. In this case, only a piece of the cylinders was used in order to ensure that the swollen cylinders still fit in the density measuring pan. The samples were weighed in air and hexane and finally put into a glass vial. The glass vial was filled with deionized water, sealed properly and placed in a dry box at 37 °C. The cylinders were weighed until equilibrium swelling was reached. For all weighings, an AT 261 balance with the appropriate density determination kit from Mettler-Toledo (Giessen, Germany) was used. A volumetric swelling ratio Q of the gels was calculated based on equations found in literature for this kind of hydrogel systems [16,23]:

$$Q = (1-\varphi)\frac{v_r}{v_s}, \tag{1}$$

where φ is the hydrogel sol fraction. The parameters v_s and v_r represent the polymer volume fraction in the hydrogel after swelling and after cross-linking but before swelling. v_s and v_r were calculated using

$$v_s = \frac{W_{a,d} - W_{n,d}}{W_{a,s} - W_{n,s}}, \tag{2}$$

and

$$v_r = \frac{W_{a,d} - W_{n,d}}{W_{a,r} - W_{n,r}}, \tag{3}$$

where $W_{a,d}$ and $W_{n,d}$ represent the weight of the cross-linked hydrogel in air or hexane after swelling and freeze drying. $W_{a,s}$ and $W_{n,s}$ correspond to the weight of the hydrogel in air or hexane after equilibrium swelling. $W_{a,r}$ and $W_{n,r}$ represent the weight of the hydrogel in air or hexane directly after cross-linking.

The hydrogel sol fraction was calculated using Eq. (4)

$$\varphi = \frac{\kappa W_{a,r} - W_{a,d}}{\kappa W_{a,r}}, \tag{4}$$

where κ represents the weight fraction of the polymer and the cross-linker in the solution prior to cross-linking. For all hydrogel formulations, κ = 0.26.

2.8. Determination of the hydrogel mesh sizes

Mesh sizes of the hydrogel networks were calculated using equations described in literature for this kind of hydrogel system [16,23]. In addition to swelling experiments, stress–strain data sets had to be recorded. In brief, data sets were recorded on a Desktop 50 universal test machine from Hegewald and Peschke (Nossen, Germany) equipped with a 20 N load cell using dog bone-shaped samples according to ASTM D638-02 type IV. All samples were swollen in water at 37 °C for several days prior to testing. Tensile testing was possible for all hydrogel formulations except the OPF10k 5% PEG-DA, which did not provide the necessary mechanical strength for testing on the used equipment. For all samples, the strain at fracture (α) as well as the strength at fracture (τ) was determined. Strain at fracture was calculated by

$$\alpha = \frac{L - L_0}{L_0}, \tag{5}$$

where L_0 and L represent the initial and final specimen length, respectively.

Table 1
Hydrogel compositions prepared by temperature-induced radical polymerization using different OPF oligomers and cross-linkers.

	Hydrogel			
	OPF3k	OPF3k 2.5% BIS	OPF3k 5% BIS	OPF10k 5% PEG-DA
OPF3k oligomer	500 mg	487.5 mg	475 mg	–
OPF10k oligomer	–	–	–	475 mg
PBS (pH 7.4)	1125 μl	625 μl	125 μl	180 μl
BIS solution (25 mg/ml)	–	500 μl	1000 μl	–
PEG-DA solution (25 mg/ml)	–	–	–	1000 μl
Ultrasound treatment ~3 min	X	X	X	X
1 N NaOH (neutralization)	75 μl	75 μl	75 μl	20 μl
Persulfate solution (82.2 mg/ml)	100 μl	100 μl	100 μl	100 μl
TEMED solution (41.8 mg/ml)	100 μl	100 μl	100 μl	100 μl
Cross-linking at 37 °C, 1 h	X	X	X	X

The molecular weights between cross-links (M_c) were calculated by

$$\frac{1}{M_c} = \frac{\tau}{\alpha - (1/\alpha^2)} \frac{Q^{\frac{1}{3}}}{RTC} + \frac{2}{M_n}, \quad (6)$$

where R represents the gas constant (8.31 kPa l/mol K), T is the temperature at which the tensile tests were conducted (293 K), C is the mass concentration of polymer in solution before cross-linking (357 g/l), and M_n is the number average molecular weight as determined by GPC (see Table 2). τ, α and Q have already been introduced before.

In order to calculate a mesh size also for the OPF10k 5% PEG-DA formulation and for comparison, the molecular weight between the cross-links (M_c) was approximated for all formulations using Eq. (6) [24].

$$M_c = \frac{n(\text{OPFxk})}{n(\text{cross-linker})} M_n(\text{OPFxk}) + M_n(\text{cross-linker}), \quad (7)$$

where n is the amount of substance either of the cross-linker or the OPF used. M_n (OPFxk) is the number average molecular weight of the OPFs according to Table 2. M_n (PEG-DA) = 575 g/mol (according to the supplier) and M_n (BIS) = 154 g/mol were used.

The mesh sizes (ξ) of the hydrogel formulations were calculated using

$$\xi = (\upsilon_s)^{-\frac{1}{3}} (\overline{r_0^2})^{\frac{1}{2}}, \quad (8)$$

where $\overline{r_0^2}$ is the end to end distance of polymer chains in the unperturbed state. $\overline{r_0^2}$ is estimated from the characteristic ratio (C_n), calculated by

$$C_n = \frac{\overline{r_0^2} M_r}{l^2 3 M_c}, \quad (9)$$

where l = 1.47 Å, the weighted average length of C–C and C–O bond lengths. C_n is taken to be 4.0 for PEG [25]. M_r is the repeating unit of the PEG chain (44 g/mol).

2.9. Characterization of the FITC-dextrans by SEC

The sizes of the 4, 40, 500 and 2000 kDa FITC-dextrans were confirmed by gel filtration chromatography (GFC) using a Shimadzu LC-System consisting of a system controller (SCL-10Avp), a pump (LC-ATvp), a degasser (DGU-14A), an autosampler (SIL-10ADvp), a column oven (CTO-10ASvp), a fluorescence detector RF-10Axl and a TSK-gel G4000SWXL column from Tosoh Bioscience GmbH (Stuttgart, Germany). About 0.5 mg of each FITC-dextran was dissolved in 6 ml purified water. Fifty microliter of these solutions were injected, and the fluorescence signal was recorded at λ_{ex} = 490 nm, λ_{em} = 520 nm for 45 min. The GFC was operated at a flow rate of 0.7 ml/min.

2.10. Characterization of FluoSpheres® by light scattering

To exclude that fluorescence of the nanoparticles distracts the light scattering experiments, their fluorescence spectra were recorded at the wavelength used for the light scattering experiment (633 nm) on a LS 55 Fluorescence Spectrometer from Perkin Elmer (Rodgau-Jügesheim, Germany). Since no measurable fluorescence signal was obtained, the samples for the size measurements were then prepared by diluting 10 µl of the FluoSpheres® stock solution (2% dispersion) with 1990 µl 1 mM NaCl. The final 0.01% Dispersion was filled in fluorescence cuvettes, and size measurements were conducted with a Zetasizer 3000 Hsa from Malvern Instruments (Herrenberg, Germany). Afterwards, the samples were diluted two times and measured again.

Table 2
Molecular weights of the PEG prepolymers and the synthesized OPFs calculated using PEG standards for calibration.

	M_w (g/mol)	M_n (g/mol)	Polydispersity (M_w/M_n)
PEG3k	2980	2493	1196
PEG10k	12,511	10,764	1162
OPF3k	8826	4517	1954
OPF10k	17,135	9964	1720

2.11. Release of FITC-dextrans and FluoSpheres®

FITC-dextrans and fluorescent polystyrene nanoparticles (FluoSpheres®, nominal bead diameter 100 nm) were used for the release experiments. The oligomer solutions according to Table 1 were prepared, but 125 µl of the PBS solution was replaced by the same amount of FITC-dextran solutions 4, 40, 500 and 2000 kDa (180 µl for the OPF10k hydrogels), or 17 µl PBS was replaced by 17 µl of the 2% FluoSpheres® solution. The amounts of fluorescent probes added to the oligomer solutions were chosen in this way to ensure a sufficient fluorescence signal during the release experiments. The solutions were filled in the same Teflon molds as described for the swelling study. The hydrogel cylinders were subsequently cut to an equal length of 10 mm and put into glass vials (n = 3). The glass vials were filled with 5 ml of PBS and maintained at 37 °C on an orbital shaker (60 rpm). At specified time intervals, 300 µl samples were taken for analysis and replaced with 300 µl fresh PBS. The released amounts of FITC-dextran (λ_{ex} = 490 nm, λ_{em} = 520 nm) and FluoSpheres® (λ_{ex} = 540 nm, λ_{em} = 560 nm) were determined using a LS55 fluorescence spectrometer from Perkin Elmer.

2.12. Confocal laser scanning microscopy of the entrapped FITC-dextrans in the hydrogels

In order to get an insight in the distribution of the FITC-dextrans inside the hydrogels, pictures were taken with a confocal laser scanning microscope LSM510 from Carl Zeiss (Jena, Germany). The samples were prepared according to Table 1, but only a fifth of all components was used, additionally 10 µl of PBS were replaced by 10 µl of a FITC-dextran solution (4, 40, 500 and 2000 kDa; 10 mg/ml). The not yet cross-linked solutions were poured into Lab-Tek™ Chamber Slides™ (Nunc™), closed, and subsequently cross-linked for 1 h in a dry box at 37 °C. Microscopic pictures were taken by exciting the sample with 1% transmission at 488 nm and collecting the emitted light through a long pass filter (505 nm) using a 10× objective with a numerical aperture of 0.3. The picture size was set to 512 Pixel × 100 Pixel and the data depth to 12 bit. The scan zoom was set to 5, the pinhole to 200 µm. After measuring the non-swollen samples, the gels were removed from the Chamber Slides™, and an appropriate amount of water, according to the swelling experiments, was added to the gels. The wet gels were then again placed in the dry box at 37 °C and allowed to swell until almost all the water was soaked up by the samples. The wet gels were then cut into appropriately sized pieces and placed back in the Chamber Slides™. Pictures were taken using the same parameters as for the non-swollen samples.

2.13. Fluorescence recovery after photobleaching (FRAP)

The diffusion of the FITC-dextrans inside the hydrogels was characterized via FRAP experiments. Samples were used analogous to those described in 2.12 in order to determine the diffusion coefficients of the dextrans. Five pictures were taken before bleaching. Afterwards, a circle with a diameter of 80 Pixel (centre at 256 Pix-

el × 50 Pixel) was bleached into the sample with three iterations using 100% transmission at all four laser wavelengths (458, 477, 488 and 512 nm). After bleaching, series of pictures were taken with parameters analogous to 2.12. The obtained fluorescence intensities of the two regions I_{whole} (512 × 100 Pixel) and I_{frap} (the bleached circle) were determined using ImageJ (National Institutes of Health, USA). The obtained data were normalized according to Eq. (7)

$$I_{frap\text{-}norm}(t) = \frac{I_{whole\text{-}pre}}{I_{whole}(t) - I_{base}(t)} * \frac{I_{frap}(t) - I_{base}(t)}{I_{frap\text{-}pre}}, \quad (7)$$

$I_{base}(t)$ is the fluorescence signal of the pure hydrogel, which could be neglected, because the blank hydrogels did not show any fluorescence at the measuring wavelength. $I_{frap\text{-}pre}$ is the normalized mean intensity of the bleached region before bleaching ($n = 5$). $I_{whole\text{-}pre}$ is the mean intensity of the whole picture before bleaching ($n = 5$). The data were further normalized to the full range using Eq. (8)

$$I_{frap\text{-}full}(t) = \frac{I_{frap\text{-}norm}(t) - I_{frap\text{-}bleach}}{I_{frap\text{-}pre} - I_{frap\text{-}bleach}}, \quad (8)$$

where $I_{frap\text{-}bleach}$ is the normalized fluorescence intensity directly after bleaching. Eq. (9) was then fitted to the normalized data involving modified Bessel functions [26]

$$f(t) = e^{\frac{-\tau_D}{2t}}\left[I_0\left(\frac{\tau_D}{2t}\right) + I_1\left(\frac{\tau_D}{2t}\right)\right], \quad (9)$$

where τ_D is the characteristic diffusion time. The diffusion coefficient was subsequently calculated using Eq. (10)

$$D = \frac{w^2}{\tau_D}, \quad (10)$$

w is the radius of the bleached spot, which was 14.4 μm for all measurements. This model is valid as long as only diffusion and no binding reactions of the fluorescent molecule to the hydrogel network take place. A correction because of the use of a scanning laser beam instead of a stationary beam was not performed.

2.14. Statistical evaluation

The obtained data were analyzed using ANOVA with subsequent Tukey test to determine statistical significances using SigmaStat 3.0.1 for Windows.

3. Results and discussion

3.1. Synthesis and characterization of OPF

The synthesized oligomers were characterized by ^{1}H NMR and GPC. The successful incorporation of the unsaturated fumarate groups in the OPF oligomers was proven by ^{1}H NMR. All synthesized oligomers showed the characteristic peak at 6.8 ppm in the ^{1}H NMR spectrum, which is attributed to the hydrogen atoms of the double bond of the fumarate group [2]. The covalent attachment of the fumarate group to the PEG units was verified by GPC as the formation of covalent bonds between the PEG units and the fumarate group concomitantly leads to higher molecular weights of the synthesized OPFs when compared to the PEGs used for the synthesis. The calculated molecular weights based on PEG standards are summarized in Table 2 for the used PEG prepolymers and for the obtained OPF oligomers. Due to the significant increase in the average molecular weight during synthesis and the observations in the ^{1}H NMR spectra, it can be concluded that the OPF oligomers synthesized for this study consist of multiple PEG units bound together via fumarate diesters and thus provide multiple double bonds that are accessible for a radical polymerization of the evenly spaced fumarate groups. Nevertheless, the observed growth of the oligomers as indicated by the obtained average molecular weights was significantly lower for OPF10k when compared to OPF3k. This difference was explained by the higher molecular weight of the used PEG10k, which is less reactive during the oligomerization with fumaryl chloride due to steric hindrance or higher molecule flexibility when compared to the significantly smaller PEG3k. This observation was also reported by Jo et al. [2] and consequently leads to a smaller degree of average oligomerization especially for the high molecular weight PEG derivatives, which can be as low as 1.5 PEG units for OPF10k, which is indicated by the integrals obtained from ^{1}H NMR (data not shown). A similar trend could be observed using the GPC, where a much wider peak was obtained for the low molecular poly(ethylene glycol) of 3 kDa, which led to significantly more high molecular weight products, which is also indicated by the polydispersity index given in Table 2.

3.2. Rheological characterization of the prepared OPF hydrogels

The synthesized OPF oligomers (OPF3k and OPF10k) were subsequently cross-linked using different types of cross-linkers (BIS, PEG-DA) and two different concentrations of BIS (2.5% and 5%) with an aqueous radical initiator system consisting of ammonium persulfate as radical initiator and TEMED as accelerator. The progress of cross-linking was followed by oscillatory rheometry. Fig. 1 shows a typical rheogram for an OPF3k oligomer solution cross-linked at 37 °C and pH 7.4.

In the first stage of the measurement (approximately 5 min), the oligomer solution behaved like a free-flowing liquid ($G'' > G'$), which is advantageous for the application, because the oligomer solution can be transferred into any kind of mold, resulting in hydrogels with specific shapes. The crossover of G' and G'' in this example at about 5 min is regarded as the gel point in literature [10] and can be used to judge the necessary cross-linking time. The cross-linking further proceeded with time as indicated in an ongoing increase in G' until a final plateau was reached ($t > 30$ min). The time needed to reach the gel point as well as the value of G' after 90 min was strongly dependent on the compositions of the used oligomer solutions. With an increasing amount of cross-linker (BIS) the time till reaching the gel point significantly decreased and additionally the stiffness of the resulting hydrogel after 90 min increased (see Table 3). The combination of OPF10k and 5% PEG-DA exhibited the lowest G' after 90 min and also the longest time period until the gel point was reached, although 5% PEG-DA was included, which is known for its enhanced reactivity when compared to the fumarate esters [27]. The big differences in cross-linking times can furthermore be explained by the longer distance between the individual cross-linking points in the oligomer of the OPF10k when compared to the OPF3k, which also leads to a reduced concentration of double bonds in the oligomer solution. The addition of the cross-linking agent PEG-DA shortens this average distance between cross-links by attributing to the overall density of unsaturated groups in the oligomer solution, but the stiffness of the resulting hydrogel still remains significantly lower when compared to the OPF3k-based gels.

3.3. Swelling behavior of the prepared OPF hydrogels

To quantify the possible degree of swelling for the different OPF hydrogels as indicator for the water uptake of the gels, the volumetric swelling ratio Q was calculated for the different gel compositions (see Table 4). Q of the different hydrogels changed conversely to the stiffness of the prepared hydrogels as the OPF10k 5% PEG-DA hydrogel exhibited the strongest swelling followed by the OPF3k and the OPF 2.5% BIS and the OPF3k 5% BIS hydrogels. Thus the swelling of the prepared gels strongly depends on the

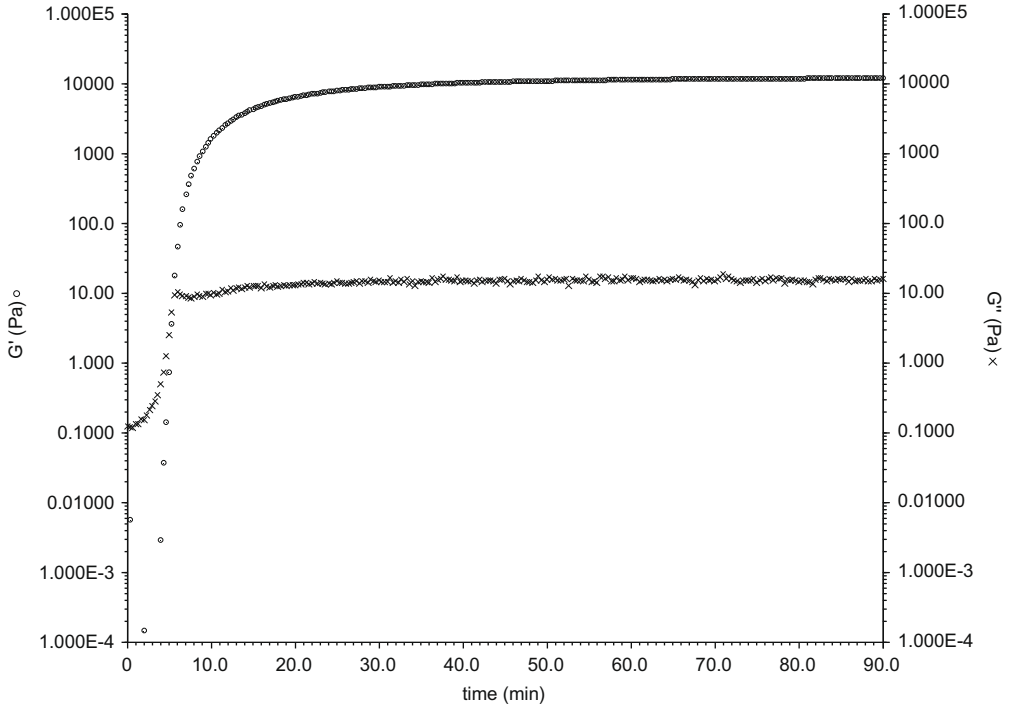

Fig. 1. Rheogram of an OPF3k oligomer solution according to Table 1 cross-linked at 37 °C and pH 7.4 (G′ ○ and G″ x). The measurement was performed at 1 Hz using a 40-mm steel plate with 1000 μm gap size.

Table 3
Rheological results for the cross-linking of the oligomer solutions according to Table 1 at 37 °C and pH 7.4 ($n = 3$).

Oligomer solution	Gel point (min)[a]	G'after 90 min (Pa)[a,b]
OPF10k 5 % PEG-DA	6.87 ± 0.61	1403 ± 72
OPF3k		
0% BIS	5.43 ± 0.06	12,127 ± 2021
2.5% BIS	1.87 ± 0.25	25,783 ± 1354
5% BIS	1.40 ± 0.10	28,717 ± 2428

[a] Data represent mean ± standard deviation, differences between the two different polymers and the individual samples for OPF3k/BIS are statistically significant.
[b] Data represent mean ± standard deviation, not statistically significant for the comparison between 2.5% and 5% BIS.

Table 4
Volumetric swelling ratio Q of the prepared hydrogels ($n = 6$) and results from mechanical testing ($n \geqslant 3$).

Oligomer solution	Vol. swelling ratio Q[a]	τ (kPa)[b]	Elongation at break α[b]
OPF10k 5% PEG-DA	17.20 ± 0.47	Not analyzable[c]	Not analyzable[c]
OPF3k			
0% BIS	4.51 ± 0.06	5.33 ± 2.31	0.33 ± 0.17
2.5% BIS	3.03 ± 0.09	12.25 ± 4.99	0.31 ± 0.13
5% BIS	2.79 ± 0.04	15.67 ± 4.93	0.33 ± 0.11

[a] Data represent mean ± standard deviation, differences between the two different polymers and the individual pairs for OPF3k/BIS are statistically significant.
[b] Data represent mean ± standard deviation, differences not statistically significant.
[c] Because of the low mechanical stability of this formulation.

OPF used and also on the amount and type of cross-linker used to adjust the mesh sizes of the hydrogels, which has been previously reported for OPF hydrogel systems [2–4,6]. Corresponding to the swelling behavior also the mesh sizes of the hydrogel could be determined for the differently cross-linked OPF gels (Table 5), with increasing amount of cross-linker added to the OPF3k gels, the calculated average mesh size decreased from 11.3 to 9.6 nm. For the even softer and more elastic OPF 10k gels the mechanical testing could not be performed, but based on the determined molecular weights, a theoretical mesh size of about 34.8 nm could be estimated (Table 5).

Table 5
Calculated mesh sizes for different OPF hydrogels with different amounts and types of cross-linking agents.

Gel type	Calculated mesh size based on M_c calculated by Eq. (7) (nm)	Calculated mesh size based on M_c calculated by Eq. (6) (nm)
OPF10k 5 % PEG-DA	34.8	Not analyzable[a]
OPF3k		
0% BIS	15.9	11.3
2.5% BIS	9.0	9.9
5% BIS	6.9	9.6

[a] Due to the lack of stability during testing of the mechanical properties.

3.4. Characterization of the particles

Two different analytical methods were used to determine the size of the used fluorescent particles depending on their individual properties. The size of the FluoSpheres® (Polystyrene beads, nominal diameter = 100 nm), was determined by light scattering. The size and integrity of the 4, 40,500 and 2000 kDa FITC-dextran was proven by GFC. The size of the FluoSpheres® was determined to be 111.2 nm ± 1.0 nm (mean ± standard deviation, calculated from measurements at three different concentrations) with a mean polydispersity index of 0.04. The used FITC-dextrans eluted at 8.9, 11.1, 16.3 and 18.6 min (4, 40, 500 and 2000 kDa) with widths at 50% height of 1.19, 2.89 and 3.79 min. The width of the peak of the FITC-dextran 2000 kDa was not calculated as it partially exceeded the exclusion limit of the used column. Nevertheless, the

used FITC-dextrans exhibited sufficiently big differences of the elution time of their maximum fluorescence with acceptable molecular weight distributions and little-detectable free dye, which made them suitable for the application as model substances for the release experiments. Based on literature values, the hydrodynamic diameter of the used FITC-dextrans (4, 40, 500 and 2000 kDa) correspond to 2.8, 9.0 [28], 31.4 and 64.6 nm [29].

3.5. Release of FluoSpheres® and FITC-dextrans from the prepared hydrogels

To investigate the release kinetics of different fluorescent nanoparticles, FluoSpheres® and FITC-dextrans (4, 40, 500 and 2000 kDa) were incorporated in the hydrogels immediately during cross-linking. All used FITC-dextrans could be released from the prepared hydrogels as indicated by the fluorescence of the release medium. The release of the FITC-dextrans was on the one hand dependent on the molecular weight of the used FITC-dextrans as indicated by a much slower release for the bigger dextrans and on the other hand also dependent on the hydrogel composition (see Table 6). The OPF10k 5% PEG-DA hydrogel generally showed the fastest release when compared to all other hydrogels except for the release of the 4 kDa FITC-dextran, where a slightly higher loading was used (180 µl FITC-dextran solution with a mass concentration of 1 mg/ml) when compared to the OPF3k hydrogel compositions (125 µl FITC-dextran solution). Because of the obviously very small size of the 4 kDa dextran, the mesh size of all prepared hydrogels seemed not to be a limiting factor for its release. That could explain why the OPF10k 5% PEG-DA hydrogel with its higher loading showed the slowest release rate for the 80% release. In contrary, the 40, 500 and 2000 kDa FITC-dextrans were always released fastest from the OPF10k 5% PEG-DA with the highest mesh sizes followed by the pure OPF3k hydrogel and the hydrogels composed of OPF3k with 2.5% and 5 % BIS added as cross-linker. The obtained typical release curves of the different dextrans from OPF3k with 2.5 % BIS are depicted in Fig. 2 and illustrate the relatively fast release of the two low molecular weight dextrans and the prolonged release of the high molecular weight derivatives. The release started without any significant burst release (all release curves started without an immediate release at time point 0) and slowly progressed dependent on the dextran's molecular weight, whereas the bigger FITC-dextrans needed more time to be released from the hydrogels than the smaller ones. At later time points for the high molecular weight dextrans, an increased variability of the release was observed, which can be attributed to slightly different onset of polymer degradation in the different investigated gel cylinders.

In contrast to the FITC-dextrans, the solid FluoSpheres® with a nominal diameter of 100 nm were not visibly released at all (released amounts below 3% for all hydrogels) from the prepared hydrogels via diffusion over a time scale of 45 h (Fig. 3). In order to exclude that the FluoSpheres® were hindered in their diffusion due to a chemical reaction with the forming hydrogel network, additionally pure OPF10k 5% PEG-DA gel cuboids were prepared, and a FluoSpheres® or methyleneblue solution as comparison were subsequently injected into the cuboids. The loaded cuboids were then placed again in PBS and were investigated for up to 2 weeks, but no obvious movement of the particles in the gel cuboids could be observed in contrast to the soluble small molecular weight methyleneblue dye (Fig. 4), which accordingly demonstrates that the observed release of below 3% can be attributed to different amounts of particles released directly from pockets in the hydrogel's outer surface.

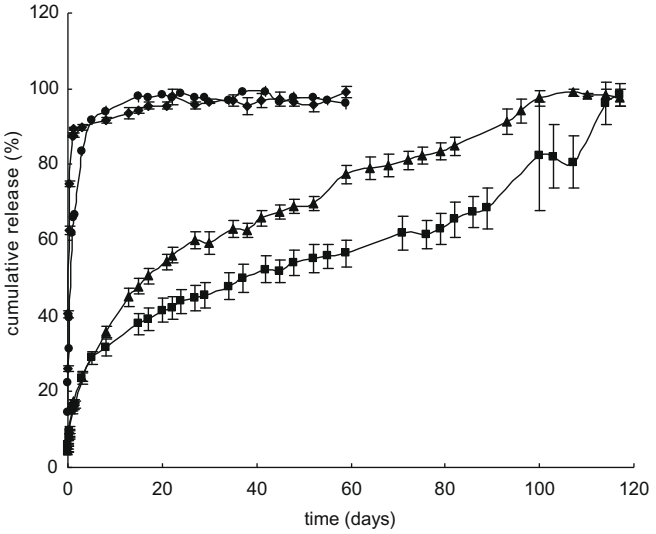

Fig. 2. Cumulative release of FITC-dextran (4 kDa -♦-, 40 kDa -●-, 500 kDa -▲- and 2000 kDa -■-) from OPF3k 2.5% BIS hydrogels. Data points represent mean ± standard deviation of three different gel cylinders.

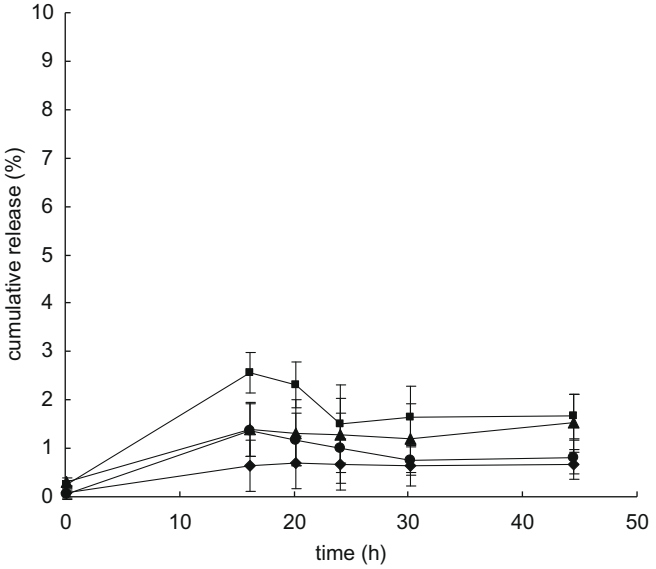

Fig. 3. Release of FluoSpheres® from differently composed hydrogel cylinders made of -♦- OPF 10k 5% PEG-DA, -▲- OPF 3k, -●- OPF 3k 2.5% Bis and -■- OPF 3k 5% Bis. Data points represent mean ± standard deviation of three different gel cylinders.

Table 6
Release times of FITC-dextrans 4, 40, 500 and 2000 kDa from the different OPF hydrogels in comparison.

Hydrogel	Release time of FITC-dextrans (time to release 80% of the final amount)			
	4 kDa	40 kDa	500 kDa	2000 kDa
OPF10k 5 % PEG-DA	8.3 h	23.4 h	12.5 days	17.5 days
OPF3k				
0% BIS	6.3 h	39.6 h	16 days	35 days
2.5% BIS	6.7 h	64.8 h	68 days	98 days
5% BIS	6.8 h	79.2 h	73.5 days[a]	99 days[a]

[a] The release was still not complete when the data collection was stopped.

3.6. Pictures of entrapped FITC-dextrans and FRAP results

To get an insight into the spatial distribution of the incorporated FITC-dextrans, microscopic pictures of the hydrogels were ta-

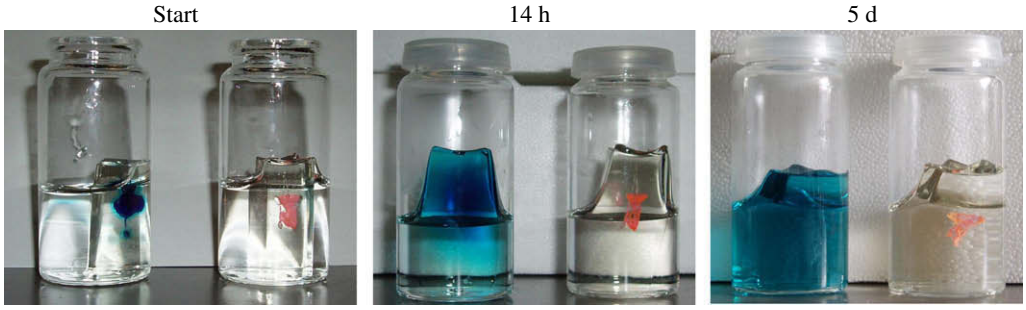

Fig. 4. Cuboids made of OPF10k-PEG-DA hydrogels loaded with methyleneblue and FluoSpheres®; observation of the dye and particle distribution over time. (For interpretation of the references to color in this figure legend, the reader is referred to the web version of this article.)

ken in the non-swollen and in the swollen state using confocal laser scanning microscopy. The FITC-dextran 4 kDa fluorescence intensity was well distributed in all hydrogel preparations in the non-swollen and in the swollen state, which further demonstrates the non-hindered diffusion throughout the hydrogel sample. The FITC-dextran 40 kDa was not homogenously distributed in the hydrogel samples in the non-swollen state, but again well distributed throughout all hydrogel samples in the swollen state. The mesh sizes of the hydrogel networks then seemed to exceed the critical size, which made it possible for the FITC-dextran to diffuse out of local conglomerates in the non-swollen state throughout the whole samples during swelling. Example pictures of the fluorescence distribution of all four FITC-dextrans (4, 40, 500 and 2000 kDa) in OPF3k hydrogels are depicted in Fig. 5. In contrast to the low molecular weight dextrans, the bigger FITC-dextrans 500 and 2000 kDa were even not homogenously distributed in the hydrogels after swelling for up to 4 days, which possibly indicates that the observed release of these two FITC-dextrans is additionally governed by a beginning degradation of the hydrogel or by a very slow hindered diffusion, which can only be elucidated by further investigations using comparable non-degradable networks based on amine-terminated poly(ethylene glycol)s.

As the two larger FITC-dextrans were not homogenously distributed in the hydrogel samples, which is necessary for the later analysis, FRAP experiments to determine the mobility of the incorporated substances were only carried out with the 4 and 40 kDa FITC-dextrans in the swollen state. The results of these FRAP experiments (see Table 7), furthermore, confirmed the results of the release experiments (see Table 6) as the 40 kDa FITC-dextran showed a much lower diffusion coefficient in the OPF3k hydrogel compositions when compared to the FITC-dextran 4 kDa. Again, for the OPF10k 5% PEG-DA sample loaded with FITC-dextran 4 kDa, the fluorescence recovery could not be appropriately analyzed due to a very fast recovery and hence a very noisy signal, which again indicates that the release rate should generally be fastest for this gel type. The calculated diffusion coefficient for the other FITC-dextran 4 kDa samples significantly decreased with an increase in the BIS concentration in the OPF3k hydrogel compositions. This effect was even stronger for the FITC-dextran 40 kDa, which is in good agreement with the results from the release experiments, where the differences observed with the lower molecular weight dextran were also much smaller due to the lower hindrance of diffusion. The difference in the release time of the smaller FITC-dextran 4 kDa between the pure OPF3k hydrogel and the OPF3k with the highest BIS concentration was only 0.5 h, whereas the difference between these two hydrogel compositions was almost 40 h for the 40 kDa FITC-dextran (see Table 6). In general, the here described FRAP experiments were suitable to judge the diffusion of

Table 7
Diffusion coefficients of the FITC-dextran-loaded OPF hydrogels in the swollen state. The diffusion coefficients were determined via fitting of Eq. (9) involving modified Bessel functions to normalized FRAP-data.

Hydrogel	Diffusion coefficient in the swollen state ($\mu m^2/s$)	
	FITC-dextran 4 kDa[b]	FITC-Dextran 40 kDa[b]
OPF10k 5% PEG-DA	Not analyzable[a]	25.72 ± 1.69
OPF3k		
0% BIS	38.43 ± 4.09	8.19 ± 0.45
2.5% BIS	25.94 ± 2.22	4.43 ± 0.10
5% BIS	22.64 ± 0.82	2.78 ± 0.16

[a] The data was not analyzable because the fluorescence recovery was too fast.
[b] Data represent mean ± standard deviation from three different measurements, all differences between individual pairs were statistically significant except for the comparison between 2.5% and 5% BIS.

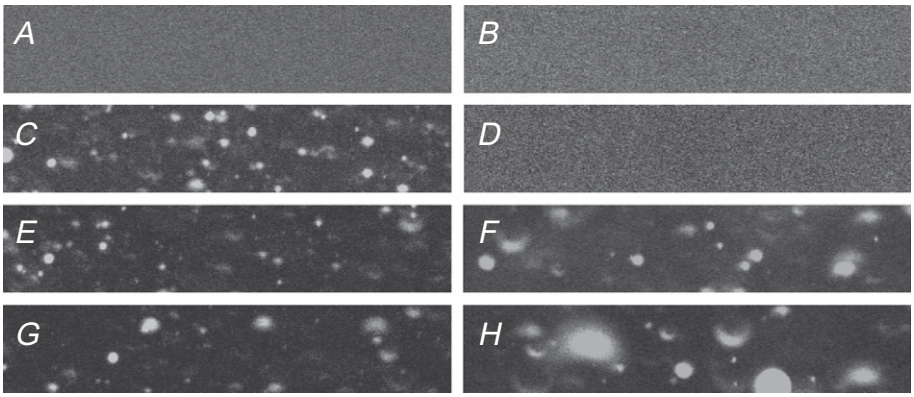

Fig. 5. FITC-dextrans 4 (A and B), 40 (C and D), 500 (E and F) and 2000 kDa (G and H) entrapped in non-swollen (A,C,E,G) and swollen (B,D,F,H) OPF3k hydrogels. All pictures 230.3 μm × 45.0 μm in size.

the different model substances and can consequently help to adjust the release system according to the desired release kinetics.

4. Conclusions

The hydrogels obtained from a temperature-induced radical polymerization of OPFs with BIS and PEG-DA as cross-linking agents were used to investigate their potential as controlled delivery system for macromolecular drugs or nanoparticles used for different delivery applications, e.g. in tissue engineering. Based on the individual mechanical and chemical properties of the used oligomers, the release kinetics could be varied in wide ranges by changing the amount of added cross-linkers or by using different PEG chain lengths for the preparation of the oligomers. The here investigated oligomers allowed a fast release up to several days for substances below 40 kDa molecular weight and a prolonged release up to several weeks or months for model substances above 500 kDa molecular weight. Further variations of the lengths of the PEG chains between the cross-linking points to lower or higher molecular weights or variations of the used cross-linkers will certainly extend the span of achievable release kinetics to slower or faster release rates. Besides the release of macromolecular dextrans, the oligomers also proved to be suited to immobilize nanoparticles of a size of 100 nm, which makes them attractive to be used as depots for encapsulated drug substances in appropriately sized particles. For the later application, the degradation of the hydrogel network has to be considered, which will additionally lead to an increased release rate of high molecular weight substances and particles, which would otherwise stay immobilized in the gel network much longer.

Application of the here described methods, release investigation and FRAP, to fluorescently labelled drug molecules, like growth factors, will furthermore allow to identify suitable hydrogel release systems with a limited amount of experiments and less protein consumption. Besides the cross-linkable oligomer-based hydrogels with different PEG lengths, the methods are obviously also applicable for other chemically cross-linked hydrogel systems, with different mesh sizes or hydrogel compositions.

Acknowledgements

The authors wish to thank the BMBF and the Bayer Schering Pharma AG for the financial support.

References

[1] F. Brandl, F. Sommer, A. Goepferich, Rational design of hydrogels for tissue engineering: impact of physical factors on cell behaviour, Biomaterials 28 (2007) 134–146.
[2] S. Jo, H. Shin, A.K. Shung, J.P. Fischer, A.G. Mikos, Synthesis and characterization of oligo(poly(ethylene glycol) fumarate) macromer, Macromolecules 34 (2001) 2839–2844.
[3] J.S. Temenoff, H. Park, E. Jabbari, D.E. Conway, T.L. Sheffield, C.G. Ambrose, A.G. Mikos, Thermally cross-linked oligo(poly(ethylene glycol) fumarate) hydrogels support osteogenic differentiation of encapsulated marrow stromal cells in vitro, Biomacromolecules 5 (2004) 5–.10.
[4] J.S. Temenoff, K.A. Athanasiou, R.G. Lebaron, A.G. Mikos, Effect of poly(ethylene glycol) molecular weight on tensile and swelling properties of oligo(poly(ethylene glycol) fumarate) hydrogels for cartilage tissue engineering, Journal of Biomedical Materials Research 59 (2002) 429–437.
[5] J.F. Lutz, Polymerization of oligo(ethylene glycol) (meth)acrylates: towards new generations of smart biocompatible materials, Journal of Polymer Science Part A 46 (2008) 3459–3875.
[6] H. Shin, S. Jo, A.G. Mikos, Modulation of marrow stromal osteoblast adhesion on biomimetic oligo[poly(ethylene glycol) fumarate] hydrogels modified with Arg-Gly-Asp peptides and a poly(ethylene glycol) spacer, Journal of Biomedical Materials Research 61 (2002) 169–179.
[7] F. Yang, C.G. Williams, D. -An Wang, H. Lee, P.N. Manson, J. Elisseeff, The effect of incorporating RGD adhesive peptide in polyethylene glycol diacrylate hydrogel on osteogenesis of bone marrow stromal cells, Biomaterials 26 (2005) 5991–5998.
[8] T. Boontheekul, D.J. Mooney, Protein-based signaling systems in tissue engineering, Current Opinion in Biotechnology 14 (2003) 559–565.
[9] R.R. Chen, D.J. Mooney, Polymeric growth factor delivery strategies for tissue engineering, Pharmaceutical Research 20 (2003) 1103–1112.
[10] F. Brandl, M. Henke, S. Rothschenk, R. Gschwind, M. Breunig, T. Blunk, J. Tessmar, A. Göpferich, Poly(ethylene glycol) based hydrogels for intraocular applications, Advanced Engineering Materials 9 (2007) 1141–1149.
[11] T.R. Hoare, D.S. Kohane, Hydrogels in drug delivery: progress and challenges, Polymer 49 (2008) 1993–2007.
[12] S.-C. Chen, Y.-C. Wu, F.-L. Mi, Yu-H. Lin, L.-C. Yu, H.-W. Sung, A novel pH-sensitive hydrogel composed of N,O-carboxymethyl chitosan and alginate cross-linked by genipin for protein drug delivery, Journal of Controlled Release 96 (2004) 285–300.
[13] D.S. Jones, C.P. Lorimer, C.P. McCoy, S.P. Gorman, Characterization of the physicochemical, antimicrobial, and drug release properties of thermoresponsive hydrogel copolymers designed for medical device applications, Journal of Biomedical Materials Research Part B: Applied Biomaterials 85B (2008) 417–426.
[14] A.A. Roos, U. Edlund, J. Sjöberg, A.-C. Albertsson, H. Stålbrand, Protein release from galactoglucomannan hydrogels: influence of substitutions and enzymatic hydrolysis by ß-Mannanase, Biomacromolecules 9 (2008) 2104–2110.
[15] D.C. Coughlan, F.P. Quilty, O.I. Corrigan, Effect of drug physicochemical properties on swelling/deswelling kinetics and pulsatile drug release from thermoresponsive poly(N-isopropylacrylamide) hydrogels, Journal of Controlled Release 98 (2004) 97–114.
[16] T.A. Holland, Y. Tabata, A.G. Mikos, In vitro release of transforming growth factor-ß1 from gelatin microparticles encapsulated in biodegradable, injectable oligo(poly(ethylene glycol) fumarate) hydrogels, Journal of Controlled Release 91 (2003) 299–313.
[17] Y.-Il Chung, K.-M. Ahn, S.-Ho Jeon, S.-Y. Lee, J.-Ho Lee, G. Tae, Enhanced bone regeneration with BMP-2 loaded functional nanoparticle-hydrogel complex, Journal of Controlled Release 121 (2007) 91–99.
[18] T.A. Holland, Y. Tabata, A.G. Mikos, Dual growth factor delivery from degradable oligo(poly(ethylene glycol) fumarate) hydrogel scaffolds for cartilage tissue engineering, Journal of Controlled Release 101 (2005) 111–125.
[19] F.K. Kasper, T. Kushibiki, Y. Kimura, A.G. Mikos, Y. Tabata, In vivo release of plasmid DNA from composites of oligo(poly(ethylene glycol)fumarate) and cationized gelatin microspheres, Journal of Controlled Release 107 (2005) 547–561.
[20] H. Park, J.S. Temenoff, Y. Tabata, A. Caplan, R.M. Raphael, J.A. Jansen, A.G. Mikos, Effect of dual growth factor delivery on chondrogenic differentiation of rabbit marrow mesenchymal stem cells encapsulated in injectable hydrogel composites, Journal of Biomedical Materials Research Part A 88A (2009) 889–897.
[21] J.S. Temenoff, H. Park, E. Jabbari, T.L. Sheffield, R.G. LeBaron, C.G. Ambrose, A.G. Mikos, In vitro osteogenic differentiation of marrow stromal cells encapsulated in biodegradable hydrogels, Journal of Biomedical Materials Research, Part A 70A (2004) 235–244.
[22] M. Dadsetan, J.P. Szatkowski, M.J. Yaszemski, L. Lu, Characterization of photo-cross-linked oligo[poly(ethylene glycol) fumarate] hydrogels for cartilage tissue engineering, Biomacromolecules 8 (2007) 1702–1709.
[23] T. Canal, N.A. Peppas, Correlation between mesh size and equilibrium degree of swelling of polymeric networks, Journal of Biomedical Materials Research 23 (1989) 1183–1193.
[24] C. Fänger, H. Wack, M. Ulbricht, Macroporous poly(N-isopropylacrylamide) hydrogels with adjustable size cut-off for the efficient and reversible immobilization of biomacromolecules, Macromolecular Bioscience 6 (2006) 393–402.
[25] F.W. Billmeyer Jr., Textbook of Polymer Science, third ed., John wiley & Sons, New York, 1984. p. 158.
[26] D.M. Soumpasis, Theoretical analysis of fluorescence photobleaching, Biophysical Journal 41 (1983) 95–97.
[27] M.D. Timmer, S. Jo, C. Wang, C.G. Ambrose, A.G. Mikos, Characterization of the cross-linked structure of fumarate-based degradable polymer networks, Macromolecules 35 (2002) 4373–4379.
[28] Product Information for fluorescein isothiocyanate dextrans, Sigma–Aldrich, downloaded March 2009
[29] K. Braeckmans, L. Peeters, N.N. Sanders, S.C. De Smedt, J. Demeester, Three-dimensional fluorescence recovery after photobleaching with the confocal scanning laser microscope, Biophysical Journal 85 (2003) 2240–2252.